

1 Orbiting Laser Configuration and Sky Coverage: Coherent 2 Reference for Breakthrough Starshot Ground-Based Laser Array

3 Eliad Peretz^a, John C. Mather^a, Christine Hamilton^a, Lucas Pabarcus^a, Kevin Hall^{a,c},
4 Robert Q. Fugate^b, Wesley A. Green^b, Peter Klupar^b

5 ^aNASA Goddard Space Flight Center, Greenbelt, MD 20771, USA

6 ^bBreakthrough Foundation

7 ^cUniversity of Maryland, 7950 Baltimore Avenue, College Park, MD, USA, 20742

8 **Abstract.** We present the concept of using an orbiting laser as a coherent optical reference to phase a several
9 kilometer diameter array of ground-based lasers designed to accelerate interstellar nano-spacecraft to 20% light-speed
10 by means of laser propulsion. We investigate the geometrical and temporal constraints for the initial case of the target
11 star Proxima b in the Alpha Centauri system using a laser ground site in the southern hemisphere. Based on these
12 constraints, we detail requirements for the mission architecture for an orbiting laser to be used as an optical reference.
13 We then present two orbits which can meet all given requirements and represent a range of engagement times and days
14 between engagements. We also present a range of orbits with periods from 3 days to 4 days and engagement times
15 from 660 to 800 seconds. *If desired, the orbit can be matched to the sidereal day, so each orbit period the beacon can*
16 *align with the ground station and the same target star without maneuvers.* A discussion of the trade off between the
17 Earth-based site latitude, time on engagement, and days between engagements is presented.

18 **Keywords:** Breakthrough Starshot, interstellar spacecraft, coherent laser array, orbiting guide star, coherent beam
19 combining .

20 *Eliad Peretz, eliad.peretz@nasa.gov

21 1 Introduction

22 The objective of the Breakthrough Starshot project is to send gram-scale spacecraft attached to a
23 meter-class light sail to nearby star systems to explore exo-solar planets. The concept is to use a
24 ground-based array of coherently combined lasers to accelerate the sail to 20% the speed of light
25 in less than 10 minutes.^{1,2} The sail and nano-craft would then coast for 22 years to reach the Al-
26 pha Centauri star system. *The sail/nano-craft would be dispensed from a mothership in a 60 Mm*
27 *orbit, then captured by the laser beam pointed toward the Alpha Centauri, offset by 77 arcseconds*
28 *to account for 26 years of proper motion of the target star, four years for Alpha Cen light to be*
29 *received and 22 for sail flight time.*³ The spatial and temporal intensity profile of the beam and the
30 design of the sail/nano-craft must be complementary so that the sail rides in the beam in a stable

31 configuration during the acceleration period.⁴⁻⁷ The current research program aims to bring this
32 concept from a technical readiness level of 1 to a proof-of-concept at 3, acknowledging that is
33 appears not to violate the laws of physics, but many challenges exist.

34

35 Phasing 100 million lasers in a close-packed array 2-3 km in diameter to produce 200 GW of
36 coherent power is an exceptionally difficult challenge.^{8,9} Arguably, the most promising phasing
37 architecture solutions involve the use of a laser reference source placed in an orbit that is very near
38 the line of propagation of the laser.¹⁰ This source provides the means to measure and correct fluc-
39 tuations in the optical path differences between apertures across the array induced by atmospheric
40 turbulence and mechanical disturbances of the optical equipment. The dual lasers of the beacon
41 require tightly controlled spectral separation, long coherence lengths and a known offset to the
42 propulsion beam wavelength. For these reasons the standard approaches to adaptive optics using
43 laser guide stars (Sodium and Rayleigh) are incompatible with this phase control concept. De-
44 tailed, comprehensive specifications of the wavelength(s), coherence properties, power, and beam
45 control parameters of the orbiting laser source won't be known until a Preliminary Design is com-
46 pleted, but a requirements envelope for range and angular position in the sky as a function of time
47 during the acceleration phase can be developed. Previous work has been done on hybrid space
48 and ground missions which can be used to align a beacon spacecraft and a ground station for an
49 astrostationary event.¹¹⁻¹⁵ These works are adapted here to show that beacon orbits are possible
50 for Starshot and meet preliminary system and mission requirements.

51

52 In this paper, we present a range of orbits which can be used to fly a laser reference source in
53 the required orbit which limits the irreparable degradations of anisoplanatism in the wavefront

54 **control system.** We describe the observational requirements for the orbit for the Breakthrough
55 Starshot mission in Section 2. These include the initial range determination **derived from focal**
56 **anisoplanatism, the field of interest derived from ordinary anisoplanatism,** the observable sky, and
57 a list summarizing all orbit requirements. In Section 3, we discuss a range of orbits which can meet
58 the stated requirements **and show the resulting Strehl reduction created by the separation between**
59 **the beacon and sail.** In Section 4 we present a discussion of those results. Finally, in Section 5 we
60 summarize the results of the paper and present future work which should be done on this topic.

61 **2 Observational Requirements**

62 *2.1 Initial Range Determination*

63 The orbiting laser needs to be at a range which reduces the effects of focal anisoplanatism.¹⁶⁻¹⁸
64 As suggested by Noyes and Hart⁸ the mean square wavefront error for a target of varying range is
65 given by the scaling law

$$\sigma_{FA}^2 = \left(\frac{D}{d_0}\right)^{\frac{5}{3}} \left(1 - \frac{R_{beacon}}{R_{sail}}\right)^{\frac{5}{3}}, \quad (1)$$

66 where D is the diameter of the ground based array, d_0 is the characteristic length associated with
67 focal anisoplanatism and depends on the C_n^2 turbulence profile and the range to the reference bea-
68 con, R_{beacon} , and R_{sail} is the range to the sail/nano-craft. Using this scaling law and the analytical
69 formula to compute d_0 ¹⁷ Figure 1 shows the effect on the Strehl ratio due only to focal anisopla-
70 natism for two beacon ranges as the sail moves from its launch point of 60 Mm to the launch end
71 point of 15,000 Mm. These results strongly suggest a minimum range for the orbiting beacon of
72 160 Mm.

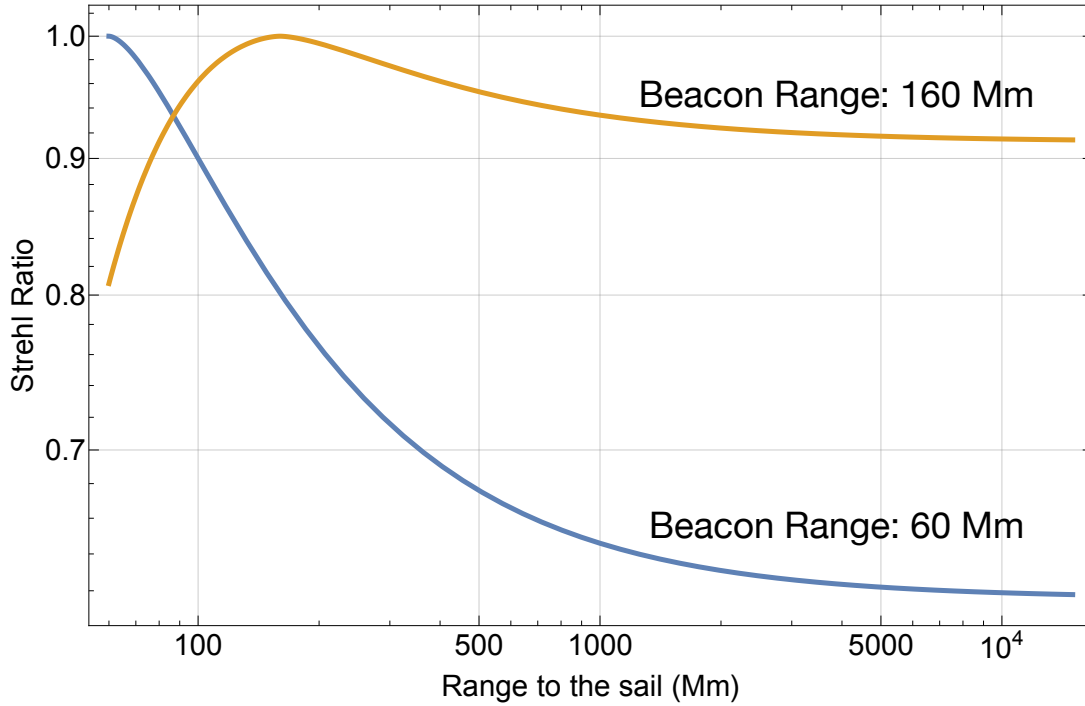


Fig 1 Focal Anisoplanatism Strehl ratio vs range to sail for two orbiting laser reference ranges. Array diameter: 3km, 1060 nm, 48 deg zenith angle, Paranal turbulence profile.¹⁹

73 *2.2 Field of interest*

74 In addition to focal anisoplanatism, losses due to angular anisoplanatism or “ordinary anisopla-
 75 natism” must be determined. The orbiting beacon will be out of the laser beam at an angle θ . A
 76 simple but useful scaling law for the anisoplanatic loss in Strehl ratio uses the Maréchal approxi-
 77 mation

$$SR_{aniso} = e^{-\sigma_{aniso}^2} \quad (2)$$

78 where

$$\sigma_{aniso}^2 = \left(\frac{\theta}{\theta_0} \right)^{5/3} \quad (3)$$

79 and where the isoplanatic angle is given by

$$\theta_0 = 0.058\lambda^{6/5}(\sec \psi)^{-8/5} \left[\int_0^\infty C_n^2(h)h^{5/3}dh \right]^{-3/5} \quad (4)$$

80 The value of the isoplanatic angle θ_0 scaled to a zenith angle of zero degrees and at a wavelength
81 of 500 nm is defined as θ_{0v} . Values of θ_{0v} range from 7 to 20 μrad for atmospheric turbulence pro-
82 files characteristic of deserts to island mountain tops, respectively. The Strehl loss due to ordinary
83 anisoplanatism for this range of conditions is plotted in Figure 2.

84 These scaling laws suggest that the off axis position of the orbiting laser beacon should be less
85 than 10 μrad for sites with excellent seeing and less than 5 μrad for sites with mediocre seeing for
86 a site in the vicinity of 30 deg south latitude.

87 2.3 Observable Sky

88 Because the engagements involve an Earth-based site, several requirements are imposed on when
89 engagements can occur. The altitude of the star must be at least 30° above the horizon. Below this
90 altitude, the air mass will be too thick, interfering with the adaptive optics. Additionally, the en-
91 gagement must be made when the sun is at least 18° below the horizon to ensure target star tracking.

92
93 Based on these ground station requirements, a map of the observable sky was created. The map
94 can be seen in Figure 3 below. More details on how this map was generated have been described

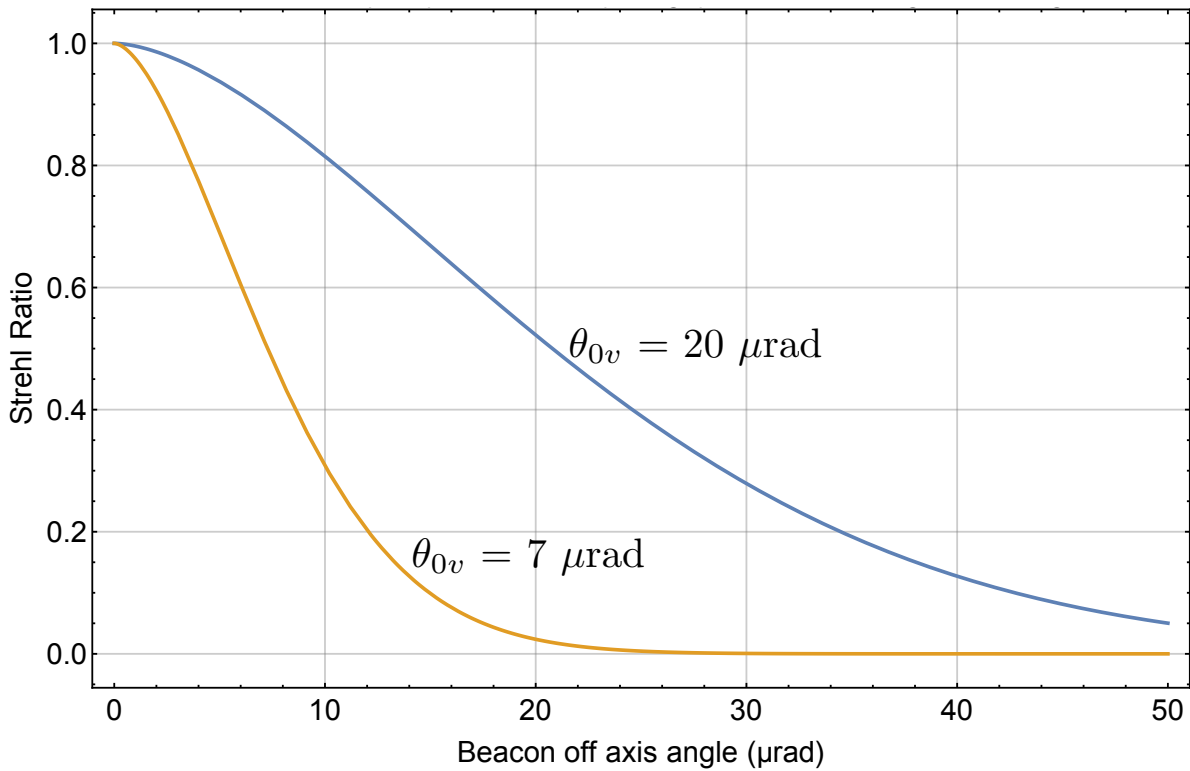


Fig 2 Strehl ratio loss due to ordinary anisoplanatism. Note: θ_{0v} is the value of θ_0 for a wavelength of 500 nm at zenith. The plot shows Strehl ratios computed for θ_0 scaled to a wavelength of 1060 nm at a zenith angle of 48 degrees.

95 previously.¹²

96 2.4 Requirements Summary

97 Table 1 lists the observational requirements for the Starshot engagement mission. These include
 98 requirements about the target star, the observation site, the times when observations can be made,
 99 and the laser.

100 The target for the mission is Proxima Centauri, which defines the target declination and right
 101 ascension for the orbit. The target proper and apparent motion is also given. The Earth-based site
 102 must be in the southern hemisphere between 25 and 65 degrees. The observable sky requirements

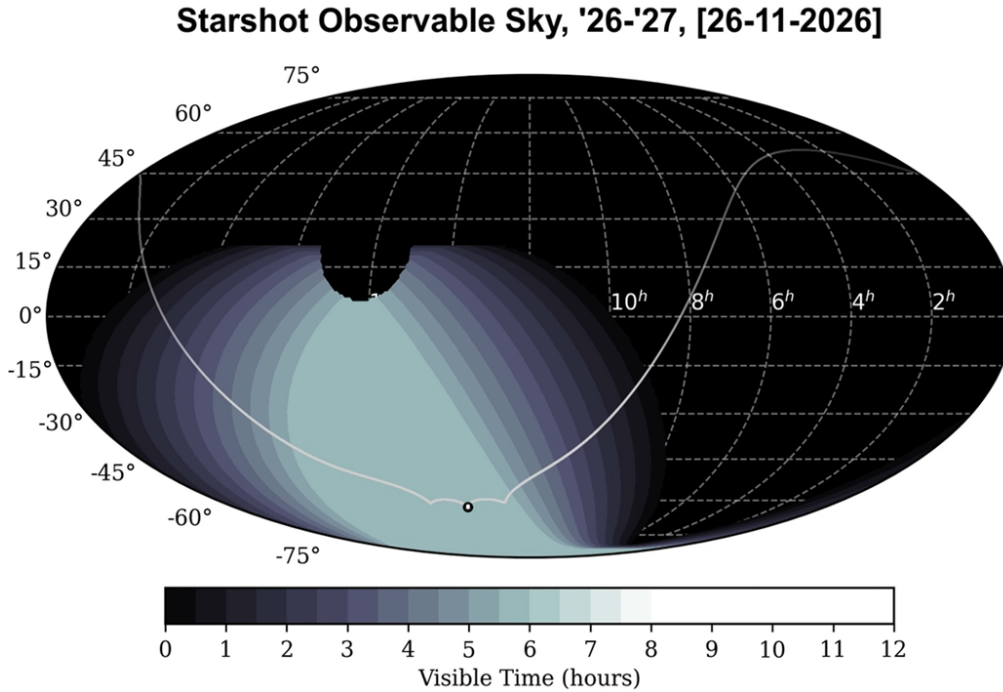


Fig 3 Observable Sky as a function of right ascension and declination, The color bar corresponds to available time due to the observational requirements (not orbit related), the white line marks the [beacon](#) trajectory as seen from the ground, the black circle dot marks the [beacon](#) location as it reaches the astro stationary observation point.

103 are also listed.

104 The Breakthrough Starshot ground laser dominates cost, expected to be of order \$10B; how-
 105 ever, the individual launches are expected to be relatively inexpensive, allowing frequent launches
 106 perhaps with redundant probe instruments to allow for launch or flight instrument casualties or
 107 suboptimal launch trajectories. A launch every two to four days is desired. The duration of launch
 108 is determined by a cost optimization model⁹ currently setting launch at 500 seconds. A longer
 109 launch of 800 seconds is given to account for future changes to the optimization model.

110 Finally, there are several requirements relating to the laser. The [orbiting](#) laser's maximum
 111 angular distance from the ground laser propagation direction during an engagement is 1 arcsecond
 112 for a 7 microradian isoplanatic angle and 2 arcseconds for a 20 microradian isoplanatic angle. In
 113 this paper, we assume a field of view of 1 arcsecond for presented results. A field of view of 2

Breakthrough Starshot Orbiting Laser Reference Observational Requirements		
Date of Information: 15 January 2021		
Item No.	Parameter	Requirement
1	Target: Proxima Centauri	
1.1	Target Coordinates	RA: 14h 29m 42.94853s DEC: -62° 40' 46.1631"
1.2	Target Proper Motion	RA: -37.81.741 mas/yr DEC: 769.465 mas/yr
1.3	Target Apparent Magnitude	10.43-11.1 (V)
2	Earth-Based Site	
2.1	Location	Southern Hemisphere
2.2	Latitude Range	25 deg S to 65 deg S
3	Engagement	
3.1	Direction	±10 deg of the meridian
3.2	Altitude	Not less than 30 deg above horizon
3.3	Time of Day	Sun more than 18 deg below the horizon
3.4	Time between Engagements	Desired: Not more than 2 days Required: Not more than 4 days
3.5	Time per Engagement	Desired: 800 seconds Required: 500 seconds
3.6	Orbiting Laser's max angular distance from ground laser propagation direction during engagement	1 arcsec for 7 microradian isoplanatic angle (Bad seeing) 2 arcsec for 20 microradian isoplanatic angle (Good seeing)
3.7	Orbiting laser's minimum angular distance from ground laser propagation direction during engagement	0.1 to 1 arcsec depending on contamination from the sail or damage to the beacon
3.8	Min Range to Orbiting Laser	160,000 km
3.9	Minimum Orbit Perigee	1000 km

Table 1 Starshot orbiting laser reference engagement requirements.

114 arcseconds would increase the engagement time available for an orbit. Next, the orbiting laser's
115 minimum angular distance from the ground laser propagation direction during an engagement
116 should be 0.1 to 1 arcsecond so that the [beacon](#) spacecraft does not block the sail and so that the
117 lasers do not directly hit the beacon satellite and damage it. Finally, the minimum range to the
118 orbiting laser is 160 million meters.

119 3 Results

120 3.1 Methods

121 Previous work has been done on designing astrostationary orbits which will allow a spacecraft to
122 inertially align with a ground station.^{13,20} Many different orbit families can be used to achieve
123 astrostationary alignment including highly elliptical and libration point orbits. Because the decli-
124 nation of the target, Proxima Centauri, is so high in this case, it would be very difficult to achieve a
125 stable orbit around a libration point that would inertially align with the target, so a highly elliptical
126 orbit was selected.

127 The development of a highly elliptical orbit to meet given astrostationary requirements has
128 previously been described¹³ but will also be reviewed here. A highly elliptical orbit allows a
129 spacecraft to inertially align with a ground station near apoapsis. At the time of engagement, the
130 spacecraft must be on the line of sight from the Earth-based site to the target, and its velocity must
131 match or be slightly below the Earth-based site.

132 Figure 4 shows the three main reference frames used in the design of this orbit. The blue frame
133 is the standard Earth Centered Inertial (ECI) frame, where $\hat{\mathbf{Z}}_{ECI}$ is aligned with the Earth's spin
134 axis and $\hat{\mathbf{X}}_{ECI}$ is aligned with the vernal equinox. The white frame is the Earth Centered Earth
135 Fixed (ECEF) frame where $\hat{\mathbf{Z}}_{\phi} = \hat{\mathbf{Z}}_{ECI}$ and $\hat{\mathbf{Y}}_{\phi}$ is aligned with the longitude of the ground station.
136 The dotted white line in the figure shows the vector from the center of the Earth to the ground
137 station. Then, the yellow dotted line shows the vector from the ground station to the target.

138 Orbits have six degrees of freedom. Two position degrees of freedom are defined by the space-
139 craft being on the line of sight from the ground station to the target at the time of engagement.
140 Next, the distance at engagement (R) can be defined by the user. This is the distance along the line

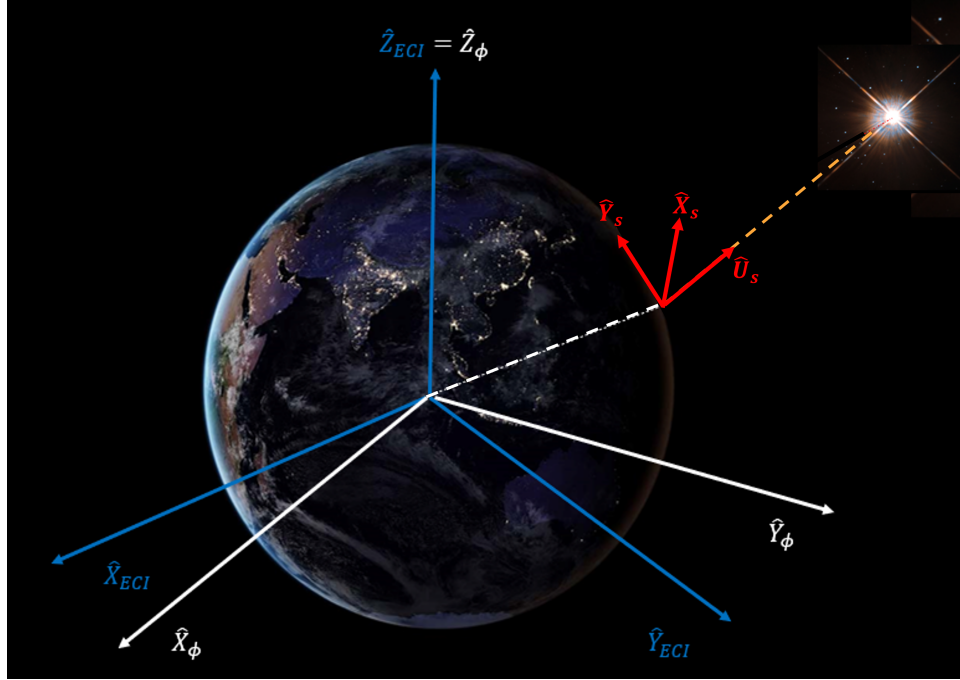


Fig 4 The key reference frames used in the development of astrostationary orbits. These include the ECI frame (blue), the ECEF frame (white), and the Isoplanatic frame (red).

141 of sight at engagement and constrains the third position degree of freedom, and it can be freely de-
 142 fined within the range of distances given by the requirements. Larger separations will give longer
 143 engagement times, but also a longer time between engagements due to a longer orbit period. At
 144 this point, the position is fully defined and the following equation can be written

$$\mathbf{r}_{ECI}^{sc} = \mathbf{r}_{ECI}^{gs} + d_{LOS} \hat{\mathbf{U}}_s \quad (5)$$

145 Note that here, the superscript *sc* refers to the **beacon** spacecraft and the superscript *gs* refers
 146 to the ground station. Similarly, two velocity degrees of freedom are defined by the fact that the
 147 velocity of the **beacon** spacecraft perpendicular to the line of sight must match the velocity of the
 148 **ground station** perpendicular to the line of sight. The third degree of freedom is defined by the user
 149 selecting the period of the orbit. For this elliptical orbit, it will be useful to choose an orbit period

150 commensurable to the sidereal day and define the semi-major axis using²¹

$$a = \frac{\mu n^2 T_{sid}^2}{(4\pi^2)^{\frac{1}{3}}} \quad (6)$$

151 Here, μ is the gravitational constant times the Earth's mass, n is the number of days in the
152 period and T_{sid} is the length of the sidereal day. Having an orbit period commensurable to the
153 sidereal day will allow for repeat observations every n days. The orbit period should be carefully
154 selected by the user, because choosing an orbit period which is too short can result in an orbit
155 which passes very close to Earth and breaks the minimum perigee requirement.

156 With these requirements, there is still one remaining binary degree of freedom. Since engage-
157 ment does not occur exactly at apogee, there are two locations on the orbit equidistant from apogee
158 when the engagement could occur. These two locations actually correspond to two different orbits
159 which are the same size and shape but are angled differently corresponding to the different time
160 in the orbit when the beacon must align with the target star. Therefore, the user must determine
161 whether the engagement will take place before apogee (an input of 1) or afterwards (an input of
162 -1). For this paper, all orbits shown have a positive velocity with an input of 1.

163 Once the design is fully constrained, the orbit position and velocity can be calculated. The
164 Vis-Viva equation is used to relate position (\mathbf{r}_{ECI}^{sc}), the semi-major axis (a), and velocity (\mathbf{v}_{ECI}^{sc})

$$\|\mathbf{v}_{ECI}^{sc}\| = \sqrt{2\mu \left(\frac{1}{\|\mathbf{r}_{ECI}^{sc}\|} - \frac{1}{2a} \right)} \quad (7)$$

165 If the orbit period is commensurable to the sidereal day, the beacon will align with the same
166 target star every n days without any maneuvers required. As stated earlier, the beacon velocity

167 perpendicular to the line of sight must be equal to the **ground station** velocity perpendicular to the
 168 line of sight, which can be expressed by

$$\mathbf{v}_{ECI,\perp}^{sc} = \mathbf{v}_{ECI}^{gs} - (\mathbf{v}_{ECI}^{gs} \cdot \hat{\mathbf{U}}_s) \hat{\mathbf{U}}_s \quad (8)$$

169 Based on this result, the velocity parallel to the line of sight can be calculated as

$$\mathbf{v}_{ECI,\parallel}^{sc} = \sqrt{\|\mathbf{v}_{ECI}^{sc}\|^2 - \|\mathbf{v}_{ECI,\perp}^{sc}\|^2} \quad (9)$$

170 The velocity of the **beacon** taken in the ECI frame is now fully defined. The chosen velocity
 171 direction determines the sign of the velocity expressed in the ECI frame parallel to the line of sight.
 172 The full definition of the velocity of the **beacon** is

$$\mathbf{v}_{ECI}^{sc} = \mathbf{v}_{ECI,\perp}^{sc} \pm (\mathbf{v}_{ECI,\parallel}^{sc}) \hat{\mathbf{U}}_s \quad (10)$$

173 With the full definition of the position and velocity, the highly elliptical orbit has been fully
 174 defined based on three user inputs: the distance along the line of sight R , the period of the orbit
 175 T , and the velocity direction (+/-1). A fourth degree of freedom is introduced in the Breakthrough
 176 Starshot mission because the ground station location has not been chosen. The ground station
 177 latitude will have an impact on the orbits which are feasible given the orbit requirements.

178 *3.1.1 Increasing Time on Target*

179 The time on target for a highly elliptical orbit can be increased by further tuning the orbit. In
 180 the original development of the orbit, the highly elliptical orbit is designed to have a velocity
 181 perpendicular to the ground station which exactly matches the ground station. Additionally, the

182 position is designed to exactly match the target star's position. However, the orbit can be further
183 optimized to significantly increase the time on target. First, if **during launch** the velocity of the
184 **beacon** perpendicular to the line of sight is slightly lower than that of the ground **ground station**, the
185 trajectory in the line of sight will become a loop rather than the peak seen previously. Additionally,
186 if the position of the observation point is moved up within the field of view this can also add time
187 in the field of view. Further detail on this process has previously been described.¹³ For the results
188 presented in this section, tuning has been done to increase the available time on target, which can
189 be seen in the looped trajectories which appear in the field of view plots presented.

190 *3.2 Possible Breakthrough Starshot Mission Orbits*

191 Based on the given requirements and the methods described for developing a highly elliptical orbit,
192 a range of orbits can be used as the orbit for the Breakthrough Starshot mission. Orbits can be
193 defined for this project by selecting a ground station latitude, a distance at the time of observation,
194 and a number of days between observations. Orbits with variations in these three parameters will
195 have different engagement times and frequency of engagements, so the desired values should be
196 used to inform the final orbit selection.

197 In the next section, we present two orbits in the available range. Both orbits meet all orbit
198 requirements, and together they give an idea of the type of orbits which can be used to meet the
199 given requirements.

200 *3.3 Example Mission Orbits*

201 Two highly elliptical orbits were developed. The first has an engagement time of 800 seconds and
202 an engagement opportunity every four days. The orbit assumes a latitude of -37.6deg, R = 199,000

203 km, and $\theta = 1$ arcsec. Figure 5 shows the orbit in the ECI frame, the orbit path in right ascension
 204 and declination, and the orbit trajectory as seen from the from the ground site's field of view.

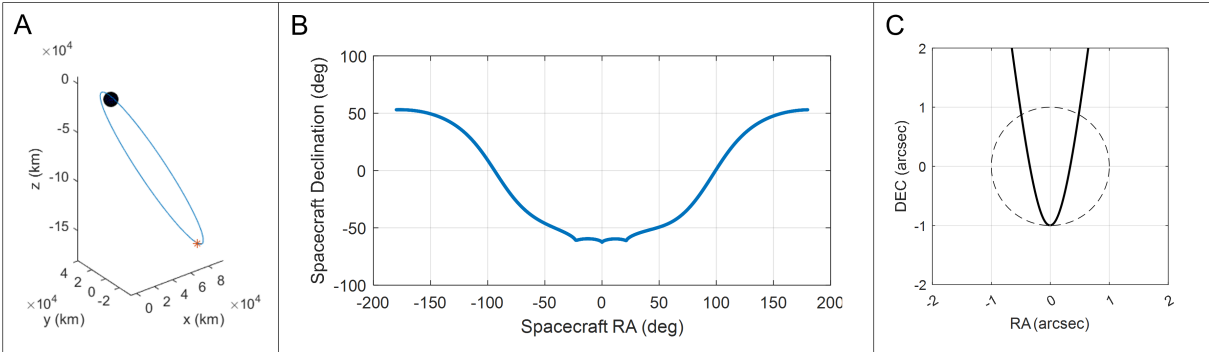


Fig 5 Results for an orbit with a latitude of -37.6deg, $R = 199,000$ km, $\theta = 1$ arcsec, and a period of 4 days. (A) The orbit in the ECI frame. (B) The **beacon spacecraft's** right ascension and declination throughout the orbit. (C) The trajectory of the orbit as seen from the telescope in the field of view. The **beacon** remains within $\theta = 1$ arcsec for 802s.

205 Tuning has been done on the orbit to increase the engagement time. In order to get the loop
 206 seen in Figure 5C, the velocity that the model is matching is 0.5 m/s slower than the ground station.
 207 Additionally, the orbit has been shifted 1 arcsecond lower in declination so that the full trajectory
 208 is captured within the field of view. As shown, the **beacon** will remain in the field of view for 802
 209 seconds.

210 Figure 6 shows the **beacon's** change in right ascension and declination over one orbit. The
 211 shaded regions show the areas where the observable sky requirements are met. As shown, the
 212 change in right ascension and declination are both less than 0.1 arcsec/s at one point, and observ-
 213 able sky requirements are met at that point. This is the location of the engagement opportunity for
 214 the orbit.

215 Given the scaling laws for ordinary and focal anisoplanatism and the parameters of a candidate
 216 orbit for the laser reference source, it is possible to estimate the losses in Strehl ratio during an
 217 engagement caused by (1) the off-axis position of the laser beacon (ordinary anisoplanatism) and

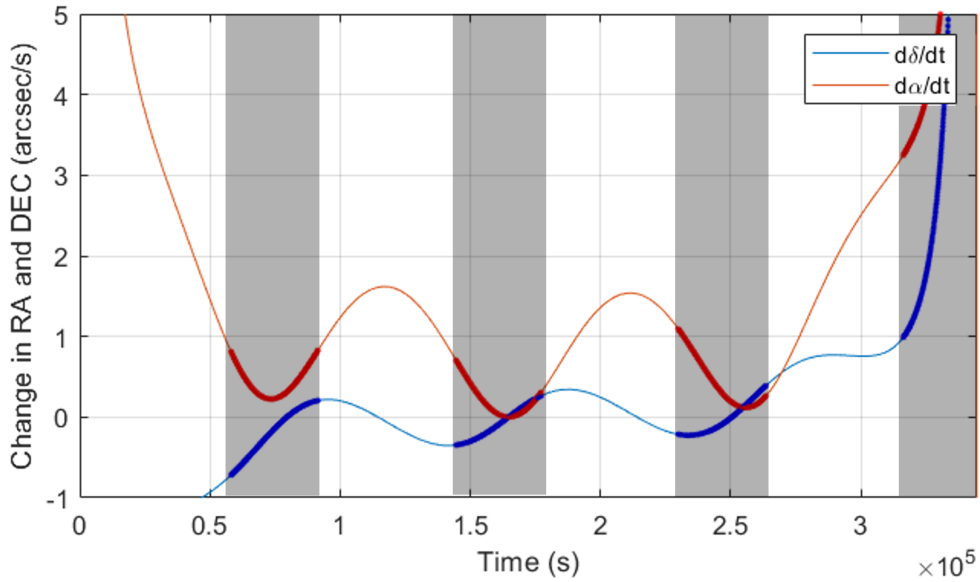


Fig 6 The beacon's change in right ascension and declination over one orbit for an orbit with a latitude of -37.6deg , $R = 199,000\text{ km}$, $\theta = 1\text{ arcsec}$, and a period of 4 days. Shaded regions show the areas where observable sky requirements are met.

218 (2) the effects of focal anisoplanatism as the sail flies out to greater ranges. The resulting Strehl
 219 model can be used to update the system model and further refine the estimates of performance.

220 Figure 7 presents results based on the candidate orbit shown in Figure 5. These results assume
 221 excellent seeing given by a Paranal C_n^2 profile but assume a more conservative value of the iso-
 222 planatic angle θ_0 of $7\ \mu\text{rad}$. The results are for a ground site at latitude 37.6 deg south making
 223 the zenith angle of the propagating launch beam 25.1 degrees ($64.9\text{ degrees elevation}$) when the
 224 engagement occurs as Proxima Centauri crosses the meridian.

225 The A panel of this figure shows the path of the orbiting laser beacon in relation to the direction
 226 of the launch beam as the black line. The angular distance to the orbiting beacon is used as an input
 227 to an angular anisoplanatism Strehl ratio computation and the results are plotted as the blue curve
 228 in Figure 7A. The blue curve shows how the Strehl ratio varies in time (top axis) measured with
 229 respect to the apogee of the beacon orbit. A launch window is defined as when the orbiting laser
 230 beacon is less than one arcsec from the launch beam. This criteria establishes an 800 second launch

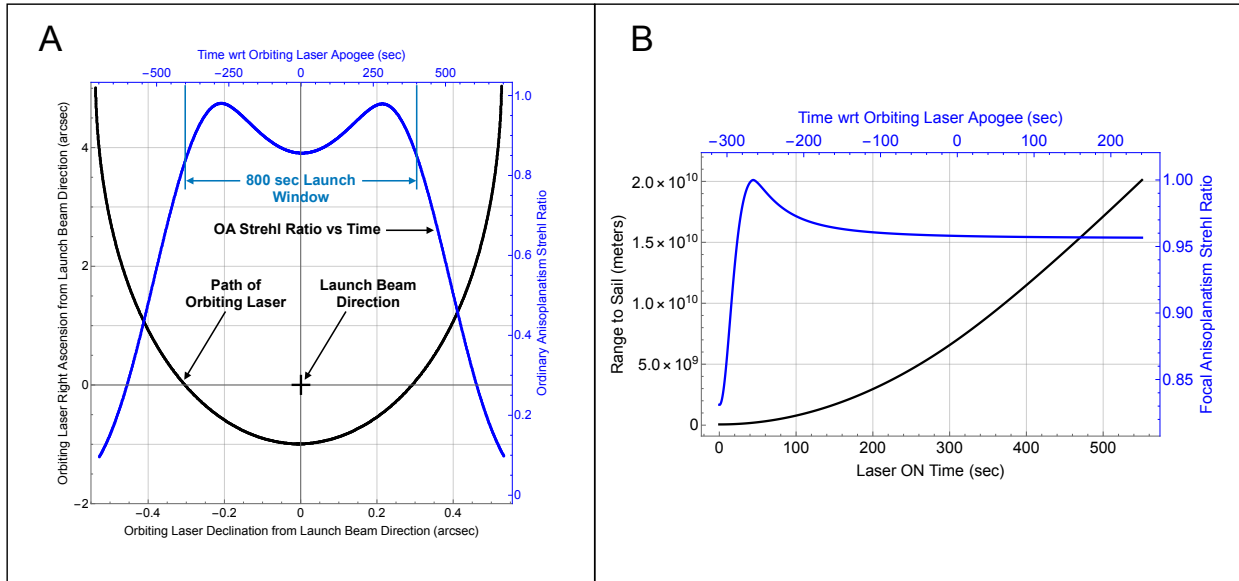


Fig 7 (A) Orbiting laser beacon path and resulting effect on launch beam Strehl ratio caused by being off axis (ordinary anisoplanatism). The black curve shows the position of the orbiting laser beacon during 1400 seconds of flight centered in time on the orbit's apogee (bottom of the curve). The blue line shows the computed Strehl ratio at each position along the orbital path as a function of time with respect to apogee. The plot show that the Strehl ratio remains above 0.85 for 800 seconds centered on the time of apogee of the orbiting laser beacon. (B) The black curve in this figure shows the range to the sail vs time while accelerating in the launch beam for 550 seconds (see text for reference). The blue curve is the computed focal anisoplanatism vs time of the launch engagement. The launch period is slightly offset from the center of the 800 second launch window shown in Figure 7A.

231 window shown centered on the plot when the angular anisoplanatism Strehl ratio has maximum
 232 values. The total time frame of the plot is 1400 seconds.

233 Figure 7B shows the effects of focal anisoplanatims on Strehl ratio as the sail flies from its
 234 starting point at 60 Mm past the orbiting laser beacon at 200 Mm with laser propulsion ending at
 235 550 seconds when the sail is at a range of 20,000 Mm and has a speed of 0.2 c. This range vs time
 236 profile was [obtained from the Parkin Model](#).⁹ The black curve displays range vs the propulsion
 237 laser on time. The blue curve shows the Strehl ratio losses from focal ansioplanatims as a function
 238 of the engagement time. The center time of the engagement is just slightly offset from the apogee
 239 time of the orbiting laser beacon to take advantage of the peak in the ordinary anisoplanatism
 240 profile.

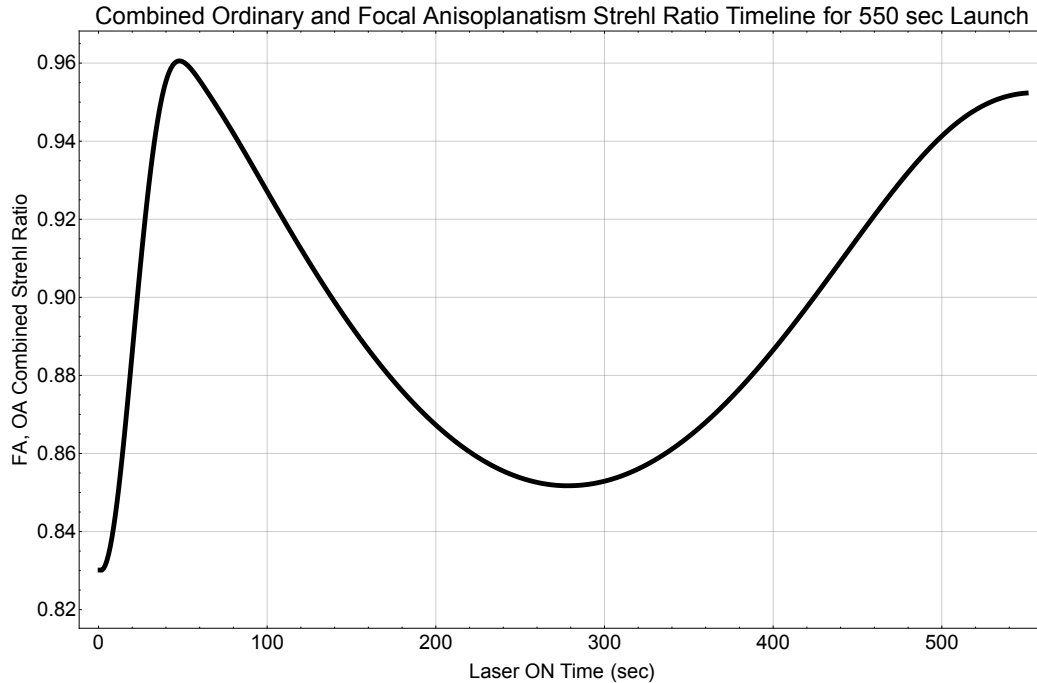


Fig 8 The combined Strehl ratio of the launch beam laser during the 550 second propagation time shown in Figure 7. As a first order estimate the Strehl ratios were combined by root sum squaring the variances. Additional discussion can be found in the text.

241 Figure 8 is a first order approximation of the combined effects of angular and focal anisopla-
 242 natism. This result was reached by computing the root sum square value of the variances given by
 243 Equation 2. These effects are not independent but interact by the fact that we are using a cone of
 244 light that is offset from the launch beam to correct a beam that is propagating through a different
 245 cone that varies with range but is on axis. Additional analyses must be completed to develop a
 246 formalism to describe this interaction between angular and focal anisoplanatism. Until that work
 247 is done we will use the root sum square of the variances. It is important to note that the curve
 248 presented in Figure 8 represents a fundamental ceiling on achievable Strehl ratio created by the use
 249 of an orbiting laser beacon for making the array of launch lasers coherent with one another while
 250 adjusting for rapid variations in optical path differences caused by phase noise in the equipment
 251 and turbulence in the atmosphere. The realization of an orbit for the laser beacon is a significant

252 step forward in the Breakthrough Starshot project.

253 This orbit is on the end of the range with a longer time between engagements but also an en-
254 gagement time of the desired 800 s. On the other hand, a second orbit was designed which would
255 allow for engagements of 700 s every 3.3 days. The orbit period was chosen based on the smallest
256 orbit which would meet perigee requirements, so orbits with less time between engagement oppor-
257 tunities will be very difficult or impossible to achieve. This orbit would have an Earth-based site at
258 a latitude of 25° , $R = 174,000$ km, and $\theta = 1$ arcsec. Figure 9 shows the orbit in the ECI frame, the
259 orbit path in right ascension and declination, and the orbit trajectory as seen from the telescope in
260 the field of view. The same orbit tuning was done on this orbit as was done on the four-day orbit.

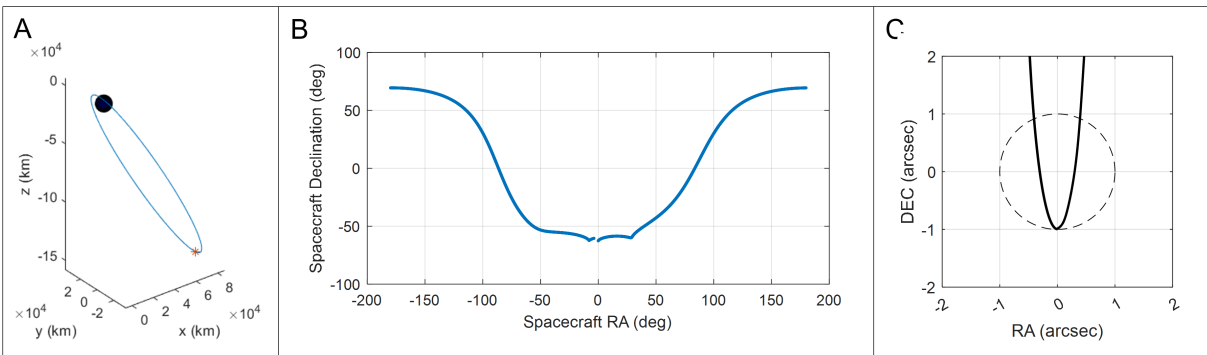


Fig 9 Results for an orbit with a latitude of -25deg , $R = 174,000$ km, $\theta = 1$ arcsec, and a period of 3.3 days. (A) The orbit in the ECI frame. (B) The **beacon**'s right ascension and declination throughout the orbit. (C) The trajectory of the orbit as seen from the telescope in the field of view. The **beacon** remains within $\theta = 1$ arcsec for 702s.

261 Figure 10 shows the **beacon**'s change in right ascension and declination over one orbit. Note
262 that since the orbit is not commensurable with an Earth day, the requirements will not be met
263 for every orbit rotation. After the first engagement the next one will occur 3.3 days later, and so
264 eventually engagements will take place during the day, breaking that requirement.

265 These are two example orbits which meet the given requirements and represent a range of other
266 possible orbits. On one end is the first orbit with a longer period and also a longer engagement

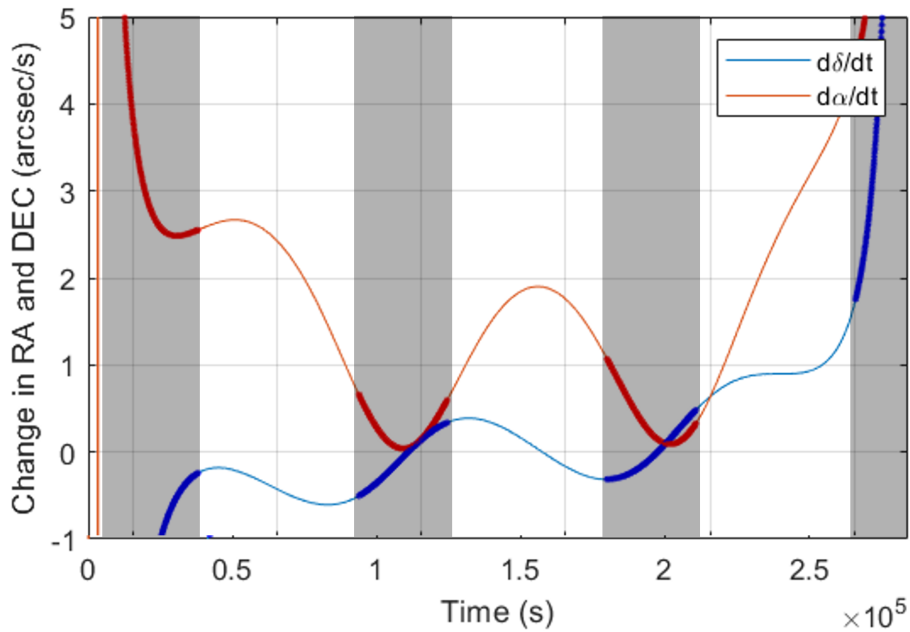


Fig 10 The **beacon**'s change in right ascension and declination over one orbit for an orbit with a latitude of -25deg, $R = 174,000$ km, $\theta = 1$ arcsec, and a period of 3.3 days. Shaded regions show the areas where observable sky requirements are met.

267 time, and on the other is the second orbit with a shorter period and a shorter engagement time.
 268 These give a sense of what types of orbits are possible for this mission.

269 The range of available orbits for this mission can be seen in Figure 11. In this figure, data is
 270 given for a range of orbit periods. Orbits were designed with periods of 3 to 4 sidereal days. For
 271 a given orbit, higher engagement times are seen with ground stations at higher latitudes. However,
 272 higher latitudes also have a lower ground station velocity, since the rotational speed of the Earth is
 273 constant. Therefore, orbits with lower periods are not possible at higher latitudes. For each orbit
 274 period, the maximum engagement time is given as well as the highest latitude that the orbit can be
 275 achieved at. Additionally, the distance from the ground station to the **beacon** at engagement is also
 276 given.

277 In the orbit requirements, the required engagement time is 500 seconds. However, at orbit
 278 periods of less than 2.9 days, the **beacon** is moving too quickly to have the velocity match that

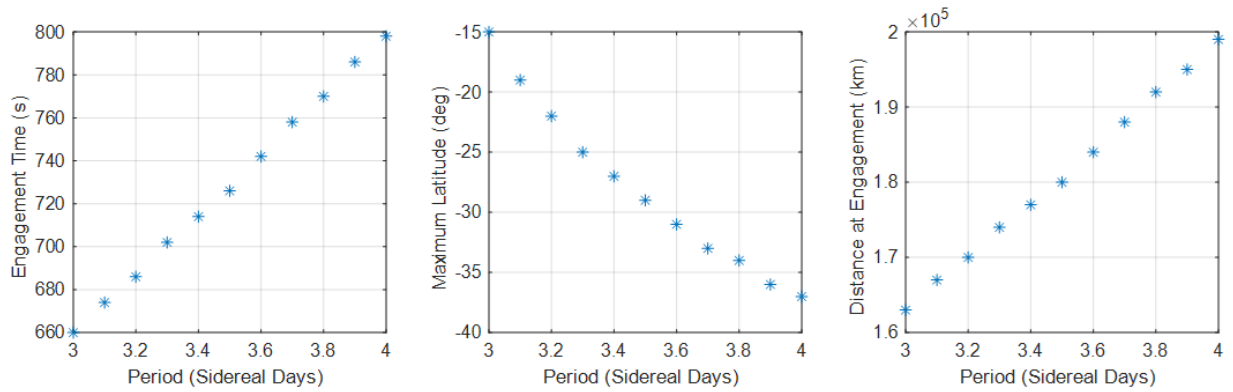


Fig 11 (Left: Orbit period in Sidereal days vs. maximum engagement time associated with the highest feasible latitude for the given orbit period. (Middle) Orbit period in sidereal days vs. highest feasible latitude. (Right) Orbit period in sidereal days vs. distance from ground station to beacon at engagement.

279 of the ground station. At that point, instead of having hundreds of seconds on the target, we
 280 have less than a minute, making those orbits infeasible for this application. Therefore, the lowest
 281 engagement time that still meets requirements will be about 650 seconds.

282 4 Discussion

283 Two possible orbits have been presented in the results section which represent a range of possible
 284 times on target and days between engagement opportunities. In order to select the orbit to be used
 285 for this mission, a preliminary design will need to be done to determine which orbit characteristics
 286 are most important.

287 A longer engagement time can be achieved by increasing the distance at engagement and/or
 288 increasing the orbit period. Additionally, the latitude of the ground station has a significant effect
 289 on the time on target. At latitudes further from the equator, the ground station has a lower velocity
 290 since the rotation of the Earth is constant for all latitudes but the distance from the axis of rotation
 291 is not. Therefore, at higher latitudes, the time on target can be higher but the orbit must have a
 292 slower velocity at observation, requiring a longer time period between observations. For the 800s

293 orbit, a latitude of -37.6° was chosen. If the [ground station](#) is at a higher latitude than this, more
294 than 4 days may be required for the time between engagement opportunities. At a lower latitude,
295 the engagement time will be shorter. For instance, for the same orbit at a latitude of -25° , the
296 engagement time will be 740s (the value of R must be reduced to about 197,000 km to make the
297 orbit possible). On the other hand, an orbit with 3.3 days between engagements would not be
298 possible at -37.6° latitude which is why that orbit is assumed a latitude of -25° .

299 If the 800s orbit is used, the Earth-based site would need to be in Chile, Argentina, Australia,
300 or New Zealand to be at the required latitude. Note that the latitude is a range, and so latitudes
301 slightly closer to the equator will also work. As they get much closer to the equator, by several
302 degrees, there will be a loss in engagement time of at least 10-20 seconds.

303 With a latitude of -25° , the shortest period between engagements is 3.3 days. However, if the
304 latitude requirement is slightly relaxed, an orbit with a period of three days could be designed to
305 meet all the other requirements. This orbit would require an Earth-based site at a latitude of -10° .

306 In addition to the latitude, there are other considerations to take into account when selecting
307 a final orbit. Both the orbits presented are within 50 km of the 1000km perigee requirement, so
308 any orbit selected should be checked to ensure that it meets the requirement. Additionally, if the
309 requirement is relaxed to 900 km or so, a slightly longer (5-10 seconds) engagement time could be
310 possible.

311 **5 Summary and Future Work**

312 A range of highly elliptical orbits can be designed to meet all requirements for the breakthrough
313 starshot mission. Two of those orbits have been presented in this paper as examples of the type of
314 orbit that can be selected for the mission.

315 Overall, the major trade off with this orbit design is between engagement time and days be-
316 tween engagements. The latitude of the site will also have a significant impact on what engagement
317 times are possible. The two orbits presented represent two ends of the spectrum of what type of
318 orbits are available, with one giving an engagement time of 800s and 4 days between opportu-
319 nities, and the other giving an engagement time of 700s and 3.3 days between engagements. It
320 was found that orbits shorter than 3.3 days cannot meet orbit requirements, specifically the perigee
321 requirement. The same is true for Earth based sites with latitudes south of -40° .

322 Past work has looked at using hybrid ground and space missions to meet goals that neither
323 could achieve alone. Using a hybrid mission for breakthrough Starshot will provide a laser refer-
324 ence source in an orbit creating small angular separation to the line of propagation for the Starshot
325 laser to limit anisoplanatism, while providing enough separation to avoid sail-beacon impacts or
326 illumination of the beacon from the propulsion beam. Combined with the effects of focal aniso-
327 planatism from cone angle differences the beacon can provide the means to measure and correct
328 fluctuations in the optical path differences due to atmospheric and mechanical turbulence. In this
329 paper, we have shown that having a laser reference beacon in this type of orbit is feasible.

330 A Preliminary Design will need to be completed before the final orbit for Breakthrough Starshot
331 can be selected. In the orbital requirements, several ranges were given with desired and required
332 times, and the range of orbits presented represents a trade off between those values. Future work
333 on this project should be done to determine the impact of different engagement times. sail mass,
334 sail speed, laser cost, optics cost and battery cost each affect the resulting cost-optimized array
335 diameter, power and launch duration.

336 6 Acknowledgments

337 *References*

- 338 1 R. L. Forward, “Roundtrip interstellar travel using laser-pushed lightsails,” *Journal of Space-*
339 *craft and Rockets* **21**(2), 187–194 (1984).
- 340 2 N. Kulkarni, P. Lubin, and Q. Zhang, “Relativistic spacecraft propelled by directed energy,”
341 *The Astronomical Journal* **155**(4) (2018).
- 342 3 S. Worden, W. Green, J. Schalkwyk, *et al.*, “Progress on the starshot laser propulsion system,”
343 *Applied Optics* (2021).
- 344 4 H. A. Atwater, A. R. Davoyan, O. Ilic, *et al.*, “Materials challenges for the starshot lightsail,”
345 *Nature Materials* (2018).
- 346 5 Z. Manchester and A. Loeb, “Stability of a light sail riding on a laser beam,” *The Astrophys-*
347 *ical Journal Letters* **837**(2), L20 (2017). Number: 2.
- 348 6 A. Shirin, E. Schamiloglu, C. Sultan, *et al.*, “Modeling and stability of a laser beam-driven
349 sail,” in *2021 American Control Conference (ACC)*, 4269–4275 (2021).
- 350 7 P. R. Srivastava and G. A. Swartzlander, “Optomechanics of a stable diffractive axicon light
351 sail,” *The European Physical Journal Plus* **135**(7), 570 (2020).
- 352 8 M. Noyes and M. Hart, “Analyzing the viability of satellite laser guide stars for breakthrough
353 starshot,” 6th International Conference on Adaptive Optics for Extremely Large Telescopes,
354 AO4ELT (2019).
- 355 9 K. L. G. Parkin, “The breakthrough starshot system model,” *Acta Astronautica* **152**, 370–384
356 (2018).

- 357 10 C. P. Bandutunga, P. G. Sibley, M. J. Ireland, *et al.*, “Photonic solution to phase sensing and
358 control for light-based interstellar propulsion,” *J. Opt. Soc. Am. B* **38**, 1477–1486 (2021).
- 359 11 E. Peretz, C. Hamilton, J. Mather, *et al.*, “Orcas–orbiting configurable artificial star mission
360 architecture,” *UV/Optical/IR Space Telescopes and Instruments: Innovative Technologies and
361 Concepts X*. **11819** (2021).
- 362 12 E. Peretz, J. Mather, L. Parbarcius, *et al.*, “Mapping the observable sky for a remote occulter
363 working with ground-based telescopes,” *Journal of Astronomical Telescopes, Instruments,
364 and Systems* **7**(1) (2021).
- 365 13 E. Peretz, C. Hamilton, J. Mather, *et al.*, “Astrostationary orbits for hybrid space and ground-
366 based observatories,” *Journal of Astronomical Telescopes, Instruments, and Systems* **8**(1)
367 (2022).
- 368 14 E. Peretz, K. McCormick, E. Moehring, *et al.*, “Orbiting configurable artificial star multi-
369 wavelength laser payload,” *Astronomical Optics: Design, Manufacture, and Test of Space
370 and Ground Systems III* **11820** (2021).
- 371 15 E. Peretz, J. C. Mather, K. Hall, *et al.*, “Exoplanet imaging scheduling optimization for an
372 orbiting starshade working with extremely large telescopes,” *Journal of Astronomical Tele-
373 scopes, Instruments, and Systems* **7**(1) (2020).
- 374 16 D. L. Fried and J. F. Belsher, “Analysis of fundamental limits to artificial-guide-star adaptive-
375 optics-system performance for astronomical imaging,” *Journal of the Optical Society of
376 America A* **11**, 277–297 (1994).
- 377 17 G. A. Tyler, “Rapid evaluation of d_0 ,” *Journal of the Optical Society of America A* **11**, 325–
378 338 (1994).

379 18 R. J. Sasiela, “Strehl ratios with various types of anisoplanatism,” *Journal of the Optical*
380 *Society of America A* **9**(8), 1398–1405 (1992).

381 19 G. Lombardi, J. Navarrete, and M. Sarazin, “Combining turbulence profiles from mass and
382 slodar: a statistical study of the evolution of the seeing at paranal,” *Proceedings of SPIE,*
383 *SPIE Astronomical Telescopes + Instrumentation* **7012**, 701221–1 – 10 (2008).

384 20 F. Patat, O. S. Ugolnikov, and O. V. Postlyakov, “Orbiting configurable artificial star (orcas)
385 for visible adaptive optics from the ground,” *Astronomy & Astrophysics* **51**, 385–393 (2006).

386 21 A. W. Koenig, S. D’Amico, E. Peretz, *et al.*, “Optimal spacecraft orbit design for inertial
387 alignment with ground telescope,” IEEE Aerospace Conference (2021).

388 **7 Biographies**

389 Author biographies are not available.

390 **List of Figures**

391 1 Focal Anisoplanatism Strehl ratio vs range to sail for two orbiting laser reference
392 ranges. Array diameter: 3km, 1060 nm, 48 deg zenith angle, Paranal turbulence
393 profile.¹⁹ 4

394 2 Strehl ratio loss due to ordinary ansioplanatism. Note: $\theta_0 v$ is the value of θ_0 for
395 a wavelength of 500 nm at zenith. The plot shows Strehl ratios computed for θ_0
396 scaled to a wavelength of 1060 nm at a zenith angle of 48 degrees. 6

397	3	Observable Sky as a function of right ascension and declination, The color bar corresponds to available time due to the observational requirements (not orbit related),	
398		the white line marks the beacon trajectory as seen from the ground, the black circle	
399		dot marks the beacon location as it reaches the astro stationary observation point.	7
400			
401	4	The key reference frames used in the development of astrostationary orbits. These	
402		include the ECI frame (blue), the ECEF frame (white), and the Isoplanatic frame	
403		(red).	10
404	5	Results for an orbit with a latitude of -37.6deg , $R = 199,000\text{ km}$, $\theta = 1\text{ arcsec}$,	
405		and a period of 4 days. (A) The orbit in the ECI frame. (B) The beacon spacecraft's	
406		right ascension and declination throughout the orbit. (C) The trajectory of the orbit	
407		as seen from the telescope in the field of view. The beacon remains within $\theta = 1$	
408		arcsec for 802s.	14
409	6	The beacon's change in right ascension and declination over one orbit for an orbit	
410		with a latitude of -37.6deg , $R = 199,000\text{ km}$, $\theta = 1\text{ arcsec}$, and a period of 4 days.	
411		Shaded regions show the areas where observable sky requirements are met.	15

412 7 (A) Orbiting laser beacon path and resulting effect on launch beam Strehl ratio
413 caused by being off axis (ordinary anisoplanatism). The black curve shows the
414 position of the orbiting laser beacon during 1400 seconds of flight centered in time
415 on the orbit's apogee (bottom of the curve). The blue line shows the computed
416 Strehl ratio at each position along the orbital path as a function of time with respect
417 to apogee. The plot show that the Strehl ratio remains above 0.85 for 800 seconds
418 centered on the time of apogee of the orbiting laser beacon. (B) The black curve
419 in this figure shows the range to the sail vs time while accelerating in the launch
420 beam for 550 seconds (see text for reference). The blue curve is the computed focal
421 anisoplanatism vs time of the launch engagement. The launch period is slightly
422 offset from the center of the 800 second launch window shown in Figure 7A. . . . 16

423 8 The combined Strehl ratio of the launch beam laser during the 550 second prop-
424 agation time shown in Figure 7. As a first order estimate the Strehl ratios were
425 combined by root sum squaring the variances. Additional discussion can be found
426 in the text. 17

427 9 Results for an orbit with a latitude of -25deg, $R = 174,000$ km, $\theta = 1$ arcsec, and
428 a period of 3.3 days. (A) The orbit in the ECI frame. (B) The beacon's right
429 ascension and declination throughout the orbit. (C) The trajectory of the orbit as
430 seen from the telescope in the field of view. The beacon remains within $\theta = 1$
431 arcsec for 702s. 18

432 10 The beacon's change in right ascension and declination over one orbit for an orbit
433 with a latitude of -25deg, $R = 174,000$ km, $\theta = 1$ arcsec, and a period of 3.3 days.
434 Shaded regions show the areas where observable sky requirements are met. 19

435 11 (Left: Orbit period in Sidereal days vs. maximum engagement time associated
436 with the highest feasible latitude for the given orbit period. (Middle) Orbit period
437 in sidereal days vs. highest feasible latitude. (Right) Orbit period in sidereal days
438 vs. distance from ground station to beacon at engagement. 20

439 **List of Tables**

440 1 Starshot orbiting laser reference engagement requirements. 8